Alexandria Engineering Journal (2016) 55, 3073–3080

HOSTED BY

ELSEVIER

Alexandria University

Alexandria Engineering Journal

www.elsevier.com/locate/aej
www.sciencedirect.com

ORIGINAL ARTICLE

Boundary layer flow of a Walter's B fluid due to a stretching cylinder with temperature dependent viscosity

Azad Hussain *, **Anwar Ullah**

Department of Mathematics, University of Science and Technology Bannu, Pakistan

Received 19 May 2015; revised 11 July 2016; accepted 25 July 2016
Available online 5 November 2016

KEYWORDS

Analytical solution;
Stretching cylinder;
Variable viscosity;
Walter's B fluid

Abstract The present investigation consists of an analytical treatment of a steady boundary layer flow of a Walter's B fluid due to a stretching cylinder with temperature dependent variable viscosity. The heat transfer analysis is also considered. With the help of usual similarity transformations the governing equations have been transformed into nonlinear ordinary differential equations and are solved by a powerful technique homotopy analysis method. Two models of variable viscosity, namely, Reynolds and Vogel's models are taken into account. The convergence is checked by plotting *h*-curves. The emerging parameters are discussed through graphs.

1. Introduction

The ratio of shear stress to the shear strain is known as viscosity. As far as literature survey is concerned a large number of investigations consist of works in which fluid viscosity is considered to be constant. In certain situations, the fluid viscosity does not remain constant. It may vary with distance, temperature or pressure. For example in coal slurries the viscosity of the fluid changes with temperature. In several thermal transport processes, the temperature distribution within the flow field does not remain uniform, i.e., the fluid viscosity may be changed noticeably if large temperature differences exist in the system. Therefore, it is highly desirable to take into account variable viscosity. Fluids that do not obey Newton's law of viscosity are called non-Newtonian fluids. Examples of non-Newtonian fluids are tomato sauce, mustard, mayonnaise, toothpaste, asphalt, lava and ice, mud slides, snow avalanches, etc. Massoudi and Christie [1] have investigated the effects of variable viscosity and viscous dissipation on the flow of a third grade fluid in a uniform pipe. They studied the numerical solutions with the help of straightforward finite difference method. They also discussed that the flow of a fluid-solid mixture is very complicated and may depend on several variables such as physical properties of each phase, size and shape of solid particles. The influence of constant and space dependent viscosity on the flow of a third grade fluid in a pipe has been studied analytically by Hayat et al. [2]. Later on, the approximate and analytical solution of non-Newtonian fluid with variable viscosity has been analyzed by Yursoy and Pakdemirili [3] and Pakdemirili and Yilbas [4]. The pipe flow of non-Newtonian fluid with variable viscosity keeping no slip

* Corresponding author.
E-mail address: azadhussainsamote@yahoo.com (A. Hussain).
Peer review under responsibility of Faculty of Engineering, Alexandria University.

http://dx.doi.org/10.1016/j.aej.2016.07.037

Table 1 Nusselt number for *Re* against *Pr*.

Re/*Pr*	0.1	0.2	0.3	0.4	0.5
0.1	1.24561	1.25054	1.85790	1.85803	1.85814
0.2	1.25071	1.26060	1.86839	1.86865	1.86887
0.3	1.25581	1.27067	1.87888	1.87927	1.87961
0.4	1.26092	1.28076	1.88938	1.88989	1.89035

Table 2 Nusselt number for *A* against *Pr*.

A/*Pr*	0.1	0.2	0.3	0.4	0.5
0.1	1.22637	1.22732	1.2282	1.22901	1.22976
0.2	1.27446	1.27637	1.27812	1.27974	1.28123
0.3	1.32287	1.32574	1.32836	1.33079	1.33303
0.4	1.37157	1.37539	1.37889	1.38212	1.38510

Table 3 Nusselt number for *A* against *Re*.

A/*Re*	0.1	0.2	0.3	0.4	0.5
0.1	1.2345	1.28843	1.34062	1.39122	1.44035
0.2	1.23523	1.28997	1.34303	1.39455	1.44464
0.3	1.23591	1.29140	1.34526	1.39762	1.44859
0.4	1.23654	1.29272	1.34732	1.40046	1.45225

Table 4 Skin friction for *A* against *Re*.

A/*Re*	0.1	0.2	0.3	0.4	0.5
0.1	−6.87921	−6.55554	−6.26807	−6.00921	−5.77344
0.2	−3.74707	−3.56905	−3.41075	−3.2682	−3.13845
0.3	−2.69331	−2.56441	−2.44969	−2.34641	−2.25246
0.4	−2.1597	−2.05575	−1.96321	−1.87991	−1.80419

and partial slip has been investigated analytically by Nadeem and Ali [5] and Nadeem et al. [6]. Recently, Nadeem and Akbar [7] studied the effects of temperature dependent viscosity on peristaltic flow of a Jeffrey-six constant fluid in a uniform vertical tube. Keeping this in mind, we are taking into account temperature dependent viscosity in our study. Stretching is another area of active research. A Newtonian fluid flow over a linear stretching surface was first time considered by Crane [8]. Various aspects of the flow for stretching surfaces have been focused in many investigations [9–17]. Wang [18] studied the steady flow of a viscous and incompressible fluid outside of a stretching hollow cylinder in an ambient fluid at rest. Motivation from abovementioned investigations leads us to consider a steady boundary layer flow of a Walter's B fluid due to a stretching cylinder with temperature dependent variable viscosity. The highly nonlinear problem is transformed into ordinary differential equations with the help of similarity transformations. Renolds and Vogel's models of temperature dependent variable viscosity are considered. The analytical solution is attained using powerful technique homotopy analysis method [6,19–26]. The physical behavior of various parameters is depicted through graphs (see Tables 1–4).

1.1. Description of the problem

Consider steady flow of an incompressible Walter's B fluid flow caused by a stretching tube of radius "a" in the axial direction, where z is the axis along the tube length and r is the axis in the radial direction. The surface of the tube is at temperature T_w and the ambient fluid temperature is T_1, where $T_w > T_1$. The governing equations are

$$\frac{\partial(rw)}{\partial z}+\frac{\partial(ru)}{\partial r}=0, \tag{1}$$

$$\rho\left(u\frac{\partial u}{\partial r}+w\frac{\partial u}{\partial z}\right)=\frac{2\eta_0}{r}\frac{\partial u}{\partial r}-\frac{2k_0}{r}u\frac{\partial^2 u}{\partial r^2}-\frac{2k_0}{r}w\frac{\partial^2 u}{\partial z\partial r}+\frac{\partial}{\partial r}\begin{pmatrix}2\eta_0\frac{\partial u}{\partial r}-2k_0u\frac{\partial^2 u}{\partial r^2}\\-2k_0w\frac{\partial^2 u}{\partial z\partial r}\end{pmatrix}-\frac{\partial}{\partial z}\begin{pmatrix}\eta_0\left(\frac{\partial u}{\partial z}+\frac{\partial w}{\partial r}\right)\\-k_0u\left(\frac{\partial^2 u}{\partial r\partial z}+\frac{\partial^2 w}{\partial r^2}\right)\\-k_0w\left(\frac{\partial^2 u}{\partial z^2}+\frac{\partial^2 w}{\partial z\partial r}\right)\end{pmatrix}-2\eta_0\frac{u}{r^2}-2k_0\frac{u^2}{r^3}-\frac{2k_0}{r^2}\frac{\partial u}{\partial z}, \tag{2}$$

$$\rho\left(u\frac{\partial w}{\partial r}+w\frac{\partial w}{\partial z}\right)$$
$$=\frac{1}{r}\begin{Bmatrix}\eta_0\left(\frac{\partial u}{\partial z}+\frac{\partial w}{\partial r}\right)\\ -k_0u\left(\frac{\partial^2 u}{\partial r\partial z}+\frac{\partial^2 w}{\partial r^2}\right)\\ -k_0w\left(\frac{\partial^2 u}{\partial z^2}+\frac{\partial^2 w}{\partial z\partial r}\right)\end{Bmatrix}+\frac{\partial}{\partial r}\begin{Bmatrix}\eta_0\left(\frac{\partial u}{\partial z}+\frac{\partial w}{\partial r}\right)\\ -k_0u\left(\frac{\partial^2 u}{\partial r\partial z}+\frac{\partial^2 w}{\partial r^2}\right)\\ -k_0w\left(\frac{\partial^2 u}{\partial z^2}+\frac{\partial^2 w}{\partial z\partial r}\right)\end{Bmatrix}$$
$$+\frac{\partial}{\partial z}\begin{Bmatrix}\eta_0\left(\frac{\partial u}{\partial z}+\frac{\partial w}{\partial r}\right)\\ -2k_0u\frac{\partial^2 w}{\partial r\partial z}\\ -2k_0w\frac{\partial^2 w}{\partial z^2}\end{Bmatrix}, \tag{3}$$

$$u\frac{\partial T}{\partial r}+w\frac{\partial T}{\partial z}=\alpha\left(\frac{\partial^2 T}{\partial r^2}+\frac{1}{r}\frac{\partial T}{\partial r}\right) \tag{4}$$

subject to the boundary conditions

$$\begin{aligned}&u=0,\quad w=w_w,\quad \text{at } r=a\\ &w\to 0,\quad T\to T_\infty,\quad \text{as } r\to\infty\end{aligned} \tag{5}$$

where u and w are the velocity components along the r and z directions respectively, and $w_w=2cz$ where c is a constant with positive value. Further α, v, ρ, T, k and μ are thermal diffusivity, the kinematic viscosity, fluid density, fluid temperature, thermal conductivity and viscosity of the fluid. The dimensionless problem which can describe the boundary flow is given by

$$\eta_0 Re\ \eta^2(ff''-f'^2)+2\eta_0\eta(f''+f''')+2A\eta f''f'''+2A(f'')^2$$
$$+4A\eta ff'''+4A\eta^2 ff''''-A\eta ff''-2A\eta f'f''=0, \tag{6}$$

$$\eta\theta''+(1+Re\ Prf)\theta'=0, \tag{7}$$

where we have used the similarity transformations

$$\eta=\left(\frac{r}{a}\right)^2,\quad u=\frac{-caf(\eta)}{\sqrt{\eta}},\quad w=2czf'(\eta),\quad \theta(\eta)=\frac{T-T_\infty}{T_w-T_\infty}. \tag{8}$$

Here prime denotes differentiation with respect to η. The dimensionless parameters used are

$$Re=\frac{ca^2}{v},\quad Pr=\frac{v}{\alpha},\quad A=\frac{k_0c}{\eta_0^*}. \tag{9}$$

where Re is Reynolds number, Pr is Prandtl number and A is Walter's B fluid parameter. The boundary conditions in dimensionless form are

$$f(1)=0,\quad f'(1)=0,\quad \theta(1)=1,\quad f'(\infty)\to 0,\quad \theta(\infty)\to 0. \tag{10}$$

2. Series solutions for Reynolds model

Here, the temperature dependent viscosity is expressed in the form

$$\eta_0=e^{-P\theta}, \tag{11}$$

which by Maclaurin series can be written as

$$\eta_0=1-P\theta+O(\theta^2). \tag{12}$$

It is worth mentioning that $M=0$ corresponds to the case of constant viscosity. Invoking above equation into Eqs. (6) and (7) one has

$$(1-P\theta)Re\ \eta^2(ff''-f'^2)+2(1-P\theta)\eta(f''+f''')+2A\eta f''f'''$$
$$+2A(f'')^2+4A\eta ff'''+4A\eta^2 ff''''-A\eta ff''-2A\eta f'f''=0, \tag{13}$$

$$\eta\theta''+(1+Re\ Prf)\theta'=0, \tag{14}$$

For HAM solution, we choose the following initial guesses:

$$f(0)=1-e^{1-\eta} \tag{14a}$$

$$\theta(0)=e^{1-\eta}, \tag{14b}$$

and linear operators

$$\mathcal{L}(f)=f'''+f'', \tag{14c}$$

$$\mathcal{L}(\theta)=\theta''+\theta'. \tag{15}$$

Zeroth order deformation problem is defined as

$$(1-q)\mathcal{L}_f\left[\bar{f}(\eta,q)-f_o(\eta)\right]=q\hbar_f N_f\left[\bar{f}(\eta,q),\bar{\theta}(\eta,q)\right], \tag{16}$$

$$(1-q)\mathcal{L}_\theta\left[\bar{\theta}(\eta,q)-\theta_o(\eta)\right]=q\hbar_\theta N_\theta\left[\bar{f}(\eta,q),\bar{\theta}(\eta,q)\right], \tag{17}$$

$$\bar{f}(\eta,q)=0,\quad \bar{\theta}(\eta,q)=1,\quad \bar{f}'(\eta,q)=1,\quad \eta=1, \tag{18}$$

$$\frac{\partial\bar{f}(\eta,q)}{\partial\eta}=0,\quad \bar{\theta}(\eta,q)=0,\quad \eta=\infty, \tag{19}$$

$$\begin{aligned}N_f\left[\bar{f}(\eta,q),\bar{\theta}(\eta,q)\right]=&(1-P\theta)Re\eta^2(ff''-f'^2)\\ &+2(1-P\theta)\eta(f''+f''')+2A\eta f''f'''\\ &+2A(f'')^2+4A\eta ff'''+4A\eta^2 ff''''\\ &-A\eta ff''-2A\eta f'f'',\end{aligned} \tag{20}$$

$$N_\theta\left[\bar{f}(\eta,q),\quad \bar{\theta}(\eta,q)\right]=\eta\theta''+(1+Re\ Prf)\theta', \tag{21}$$

where $q\epsilon[0,1]$ is the embedding parameter and $\hbar_f$ and $\hbar_\theta$ are auxiliary non-zero operators.

The mth order deformation equations are defined as

$$\mathcal{L}_f[f_m(\eta)-\chi_m f_{m-1}(\eta)]=\hbar_f R_f(\eta), \tag{22}$$

$$\mathcal{L}_\theta[\theta_m(\eta)-\chi_m\theta_{m-1}(\eta)]=\hbar_\theta R_\theta(\eta), \tag{23}$$

where

$$\chi_m=\begin{cases}0, & m\leqslant 1,\\ 1, & m>1.\end{cases} \tag{24}$$

and

$$R_f(\eta)=Re\ \eta^2(ff''-f'^2)-P\theta Re\eta^2(ff''-f'^2)+2\eta(f''_{m-1}+f'''_{m-1})$$
$$-2P\eta\begin{pmatrix}\sum_{k=0}^{m-1}f''_{m-1-k}\theta_k\\ +\sum_{k=0}^{m-1}f'''_{m-1-k}\theta_k\end{pmatrix}+2A\eta\sum_{k=0}^{m-1}f''_{m-1-k}f'''_k$$
$$+2A\sum_{k=0}^{m-1}f'_{m-1-k}f''_k+4A\eta\sum_{k=0}^{m-1}f'_{m-1-k}f'''_k+4A\eta^2\sum_{k=0}^{m-1}f'_{m-1-k}f''''_k$$
$$-A\eta\sum_{k=0}^{m-1}f_{m-1-k}f''_k-2A\eta\sum_{k=0}^{m-1}f'_{m-1-k}f''_k, \tag{25}$$

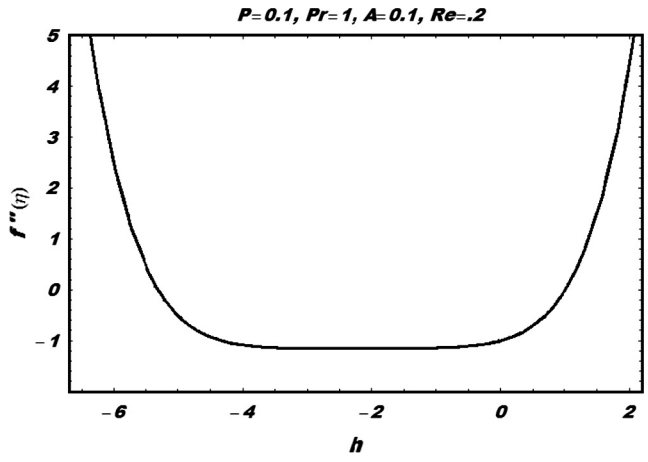

Figure 1 *h*-curve for velocity profile for Reynolds model.

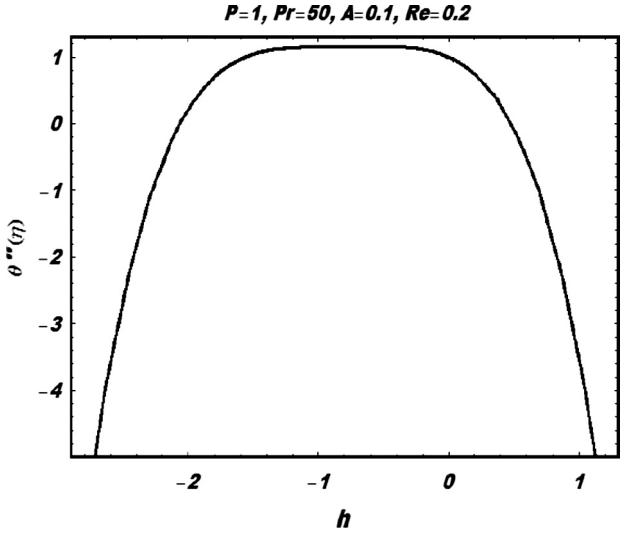

Figure 2 *h*-curve for temperature profile for Reynolds model.

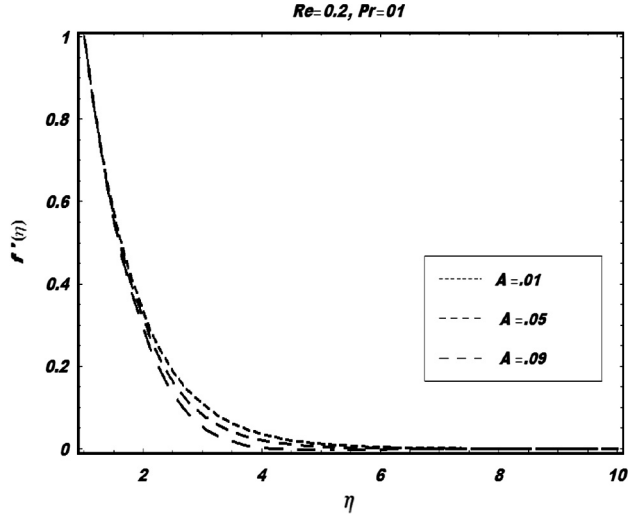

Figure 3 Velocity profile for different values of A for Reynolds model.

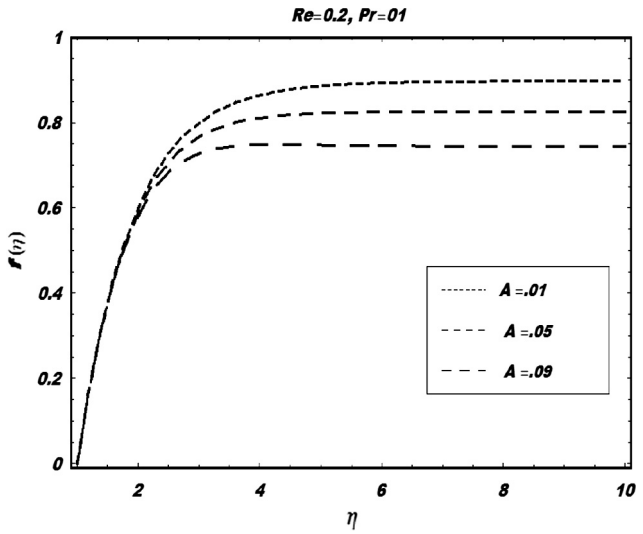

Figure 4 f(η) profile for different values of A for Reynolds model.

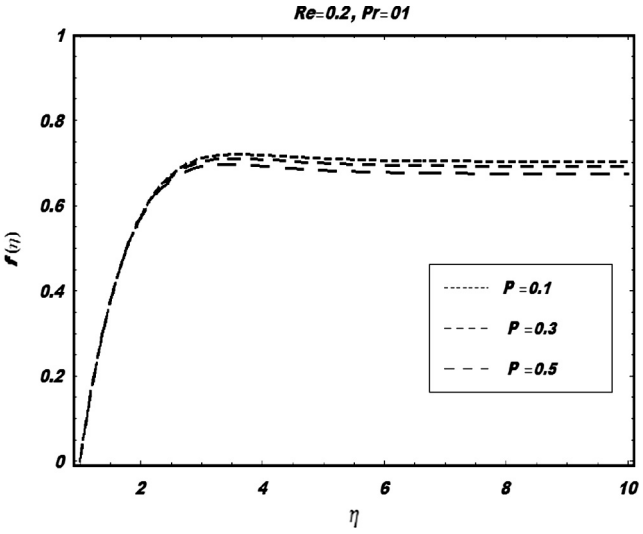

Figure 5 f(η) profile for different values of P for Reynolds model.

$$R_\theta(\eta) = \eta\theta''_{m-1} + \theta'_{m-1} + Re\ Pr\sum_{k=0}^{m-1} f_{m-1-k}\theta'_k. \tag{26}$$

We now use the symbolic software MATHEMATICA and solve the set of linear differential Eqs. (25) and (26) subject to relevant boundary conditions up to first few order of approximations. It is found that $f_m(\eta)$ and $\theta_m(\eta)$ can be written as

$$\begin{aligned} f_m(\eta) &= \sum_{n=0}^{2m}\sum_{l=0}^{m} b_{m,n}\eta^n e^{l-n\eta}, \\ \theta_m(\eta) &= \sum_{n=1}^{m}\sum_{l=0}^{m} d_{m,n}\eta^{2(n-1)} e^{l-(2n+1)\eta}, \quad m \geqslant 0. \end{aligned} \tag{27}$$

The solution thus can be defined as

$$f(\eta) = \lim_{Q\to\infty}\left[\sum_{m=0}^{Q}\left(\sum_{n=0}^{2m}\sum_{l=0}^{m} b_{m,n}\eta^n e^{l-n\eta}\right)\right], \tag{28}$$

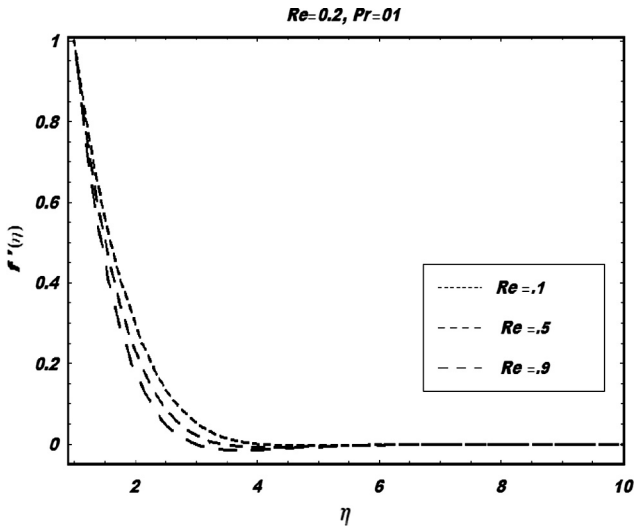

Figure 6 Velocity profile for different values of *Re* for Reynolds model.

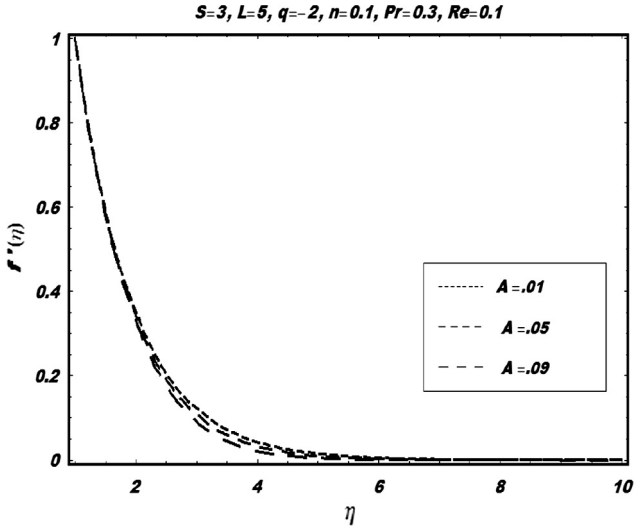

Figure 7 Velocity profile for different values of *A* for Vogel's model.

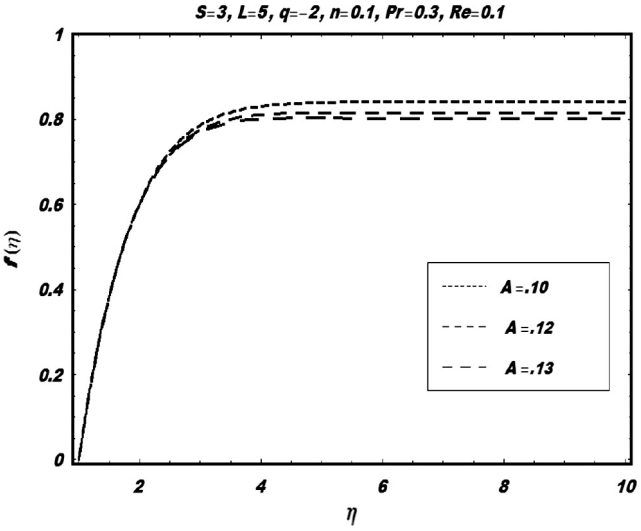

Figure 8 f(η) profile for different values of *A* for Vogel's model.

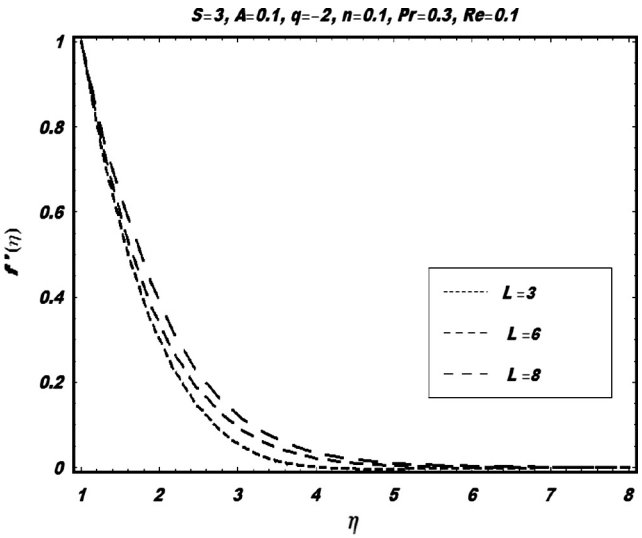

Figure 9 Velocity profile for different values of *L* for Vogel's model.

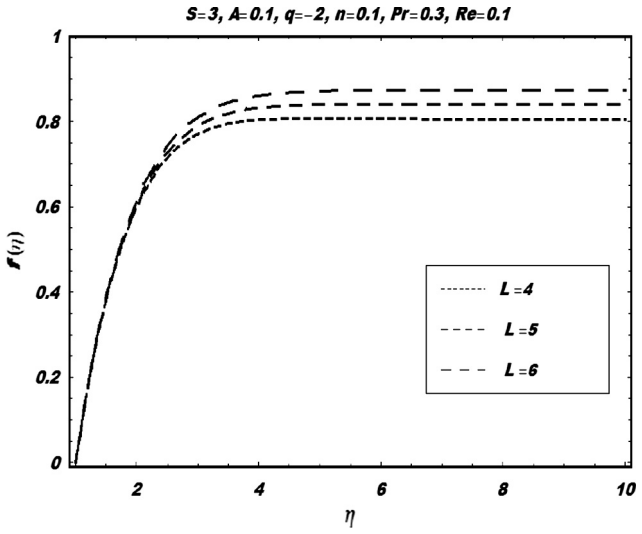

Figure 10 f(η) profile for different values of *L* for Vogel's model.

$$\theta(\eta) = \lim_{Q\to\infty}\left[\sum_{m=0}^{Q}\left(\sum_{n=1}^{m}\sum_{l=0}^{m} d_{m,n}\eta^{2(n-1)}e^{l-(2n+1)\eta}\right)\right]. \tag{29}$$

3. Series solutions for Vogel's model

Here

$$\eta_0 = \eta_0^* \exp\left[\frac{n}{(q+\theta)} - \theta_0\right], \tag{30}$$

which by Maclaurin series reduces to

$$\eta_0 = \frac{L}{S}\left(1 - \frac{\theta n}{q^2}\right) \quad \text{where} \quad S = \eta_0^* \exp\left[\frac{n}{q} - \theta_0\right]. \tag{31}$$

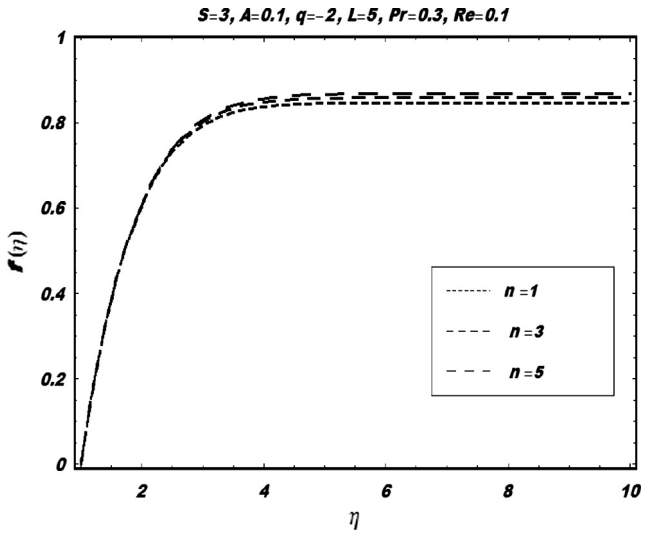

Figure 11 f(η)) profile for different values of n for Vogel's model.

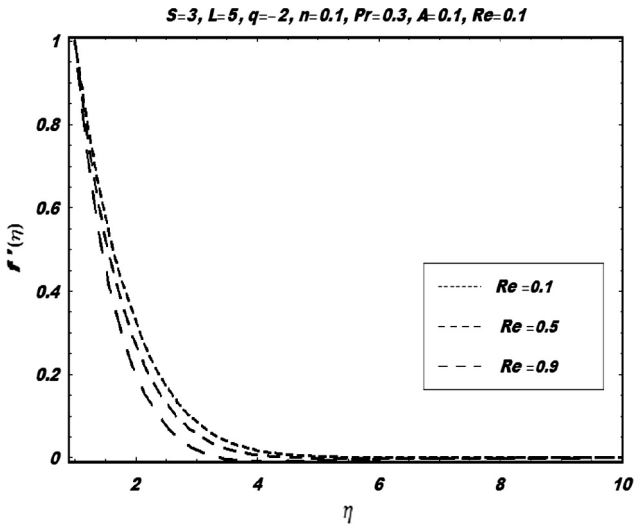

Figure 13 Velocity profile for different values of Re for Vogel's model.

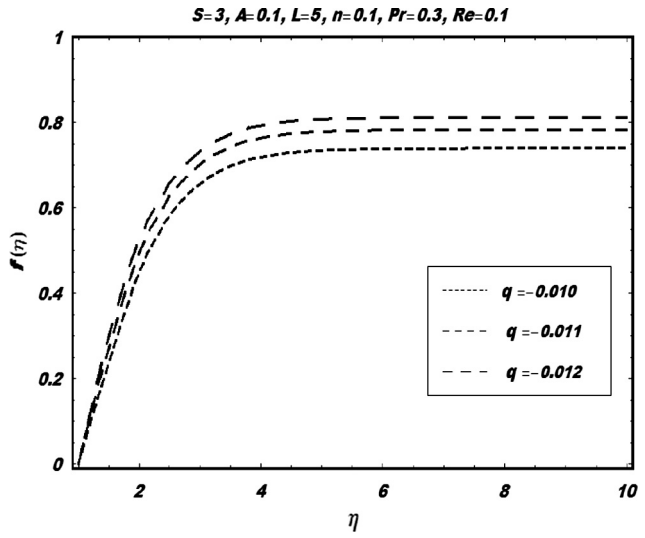

Figure 12 f(η) profile for different values of q for Vogel's model.

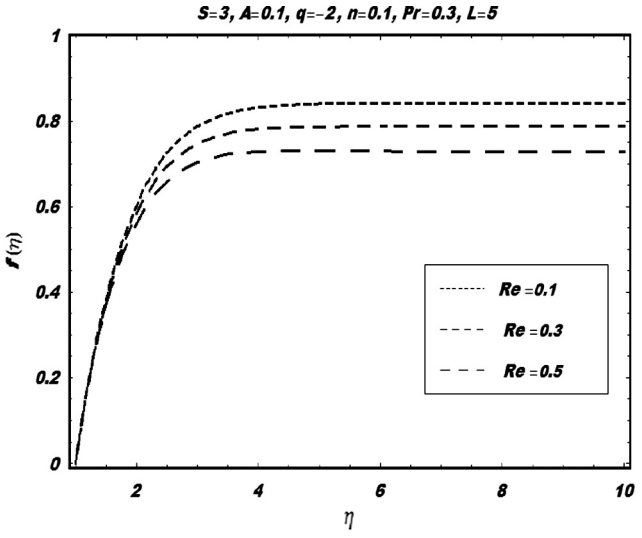

Figure 14 f(η) profile for different values of Re for Vogel's model.

Invoking above expression, Eqs. (6) and (7) become

$$\frac{L}{S}\left(1-\frac{\theta n}{q^2}\right)Re\eta^2(ff''-f'^2)+2\frac{L}{S}\left(1-\frac{\theta n}{q^2}\right)\eta(f''+f''')+2A\eta f''f'''+2A(f'')^2+4A\eta ff'''+4A\eta^2 ff''''-A\eta ff''-2A\eta f'f''=0, \tag{32}$$

$$\eta\theta''+(1+Re\ Prf)\theta'=0, \tag{33}$$

Using the similar procedure as discussed in previous section, the solution of this case is straightforward written as

$$f_m(\eta)=\sum_{n=0}^{2m}\sum_{l=0}^{m}a'_{m,n}\eta^n e^{l-n\eta},$$
$$\theta_m(\eta)=\sum_{n=1}^{m}\sum_{l=0}^{m}b'_{m,n}\eta^{2(n-1)}e^{l-(2n+1)\eta},\quad m\geqslant 0, \tag{34}$$

where $a'_{m,n}$ and $b'_{m,n}$ are constants.

4. Graphical results and discussion

In order to report the convergence of the obtained series solutions and the effects of sundry parameters in the present investigation we plotted Figs. 1–19. Figs. 1 and 2 are prepared to see the convergence region. Fig. 3 shows the velocity variation for different values of A for Renolds model. It can be seen that velocity decreases as A increases. Fig. 4 shows f(η) profile for different values of A for Reynolds model. Fig. 5 is plotted to see f(η) profile for different values of P for Reynolds model. Fig. 6 depicts velocity profile for different values of Re for Renolds model. We see that with increase in Re velocity profile is decreased. Fig. 7 depicts velocity profile for different values of A for Vogel's model. It is to be noted that velocity profile is

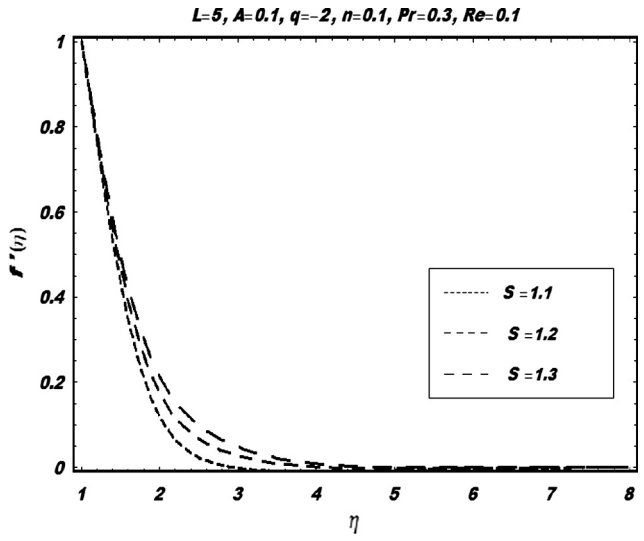

Figure 15 Velocity profile for different values of S for Vogel's model.

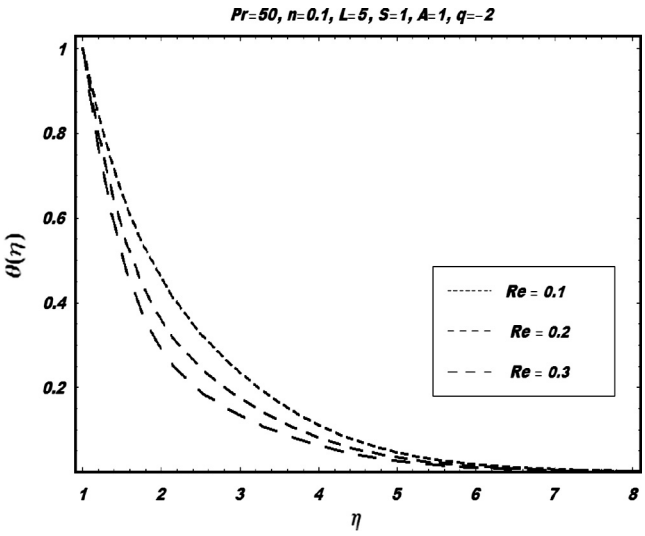

Figure 17 Temperature profile for different values of Re for Vogel's model.

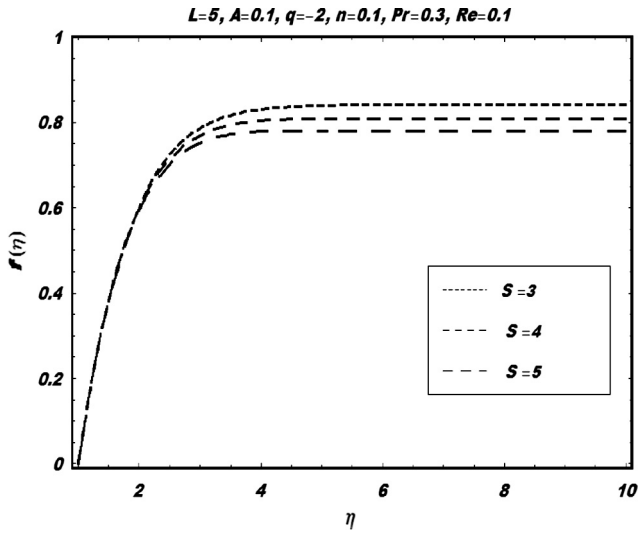

Figure 16 f(η) profile for different values of S for Vogel's model.

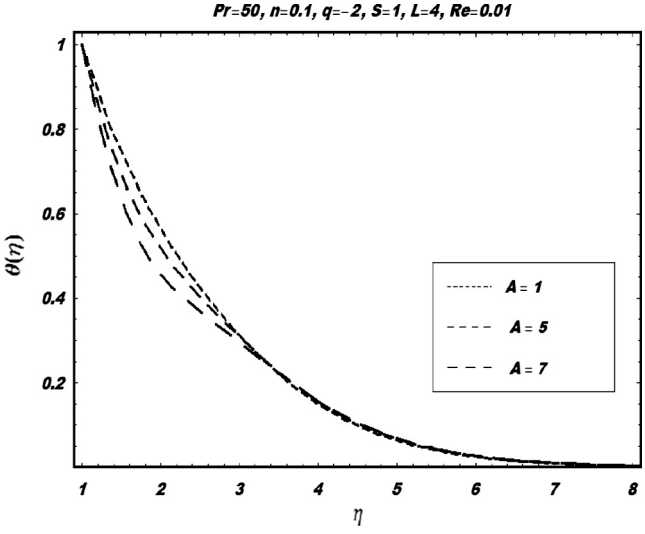

Figure 18 Temperature profile for different values of A for Vogel's model.

decreased with increase in A. Fig. 8 shows f(η) profile for different values of A for Vogel's model. Fig. 9 shows velocity profile for different values of L for Vogel's model. Velocity profile for different values of L for Vogel's model is increased with increase in L. Fig. 10 shows f(η) profile for different values of L for Vogel's model. Fig. 11 is plotted to see f(η) profile for different values of n for Vogel's model. Fig. 12 shows the f(η) profile for different values of q for Vogel's model. Fig. 13 depicts velocity profile for different values of Re for Vogel's model. It is observed that velocity profile decreases with increase in Re. Fig. 14 shows f(η) profile for different values of Re for Vogel's model. Fig. 15 depicts velocity profile for different values of S for Vogel's model. It is depicted that velocity increases as S increases. Fig. 16 is plotted to see the f(η) profile for different values of S for Vogel's model. Fig. 17 reveals temperature profile for different values of Re for Vogel's model. It is seen that temperature decreases as

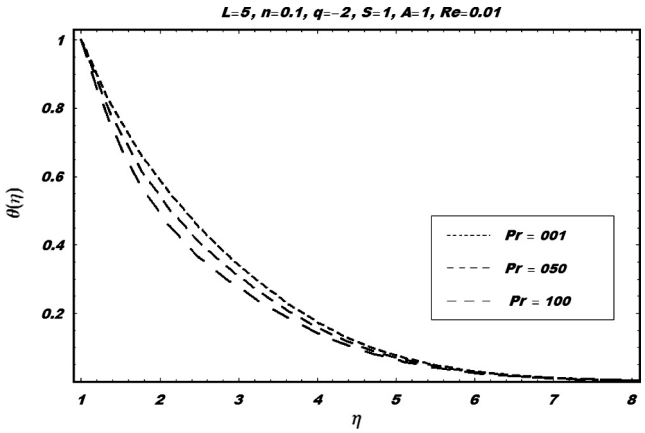

Figure 19 Temperature profile for different values of Pr for Vogel's model.

Re increases. Fig. 18 presents temperature profile for different values of *A* for Vogel's model. It is observed that temperature decreases as *A* increases. Fig. 19 depicts temperature profile for different values of *Pr* for Vogel's model. It is seen that temperature decreases as *Pr* increases.

4.1. Conclusions

In this paper, we have investigated analytically the heat transfer flow of a Walter's B fluid due to a stretching cylinder. Using usual similarity transformations the governing equations have been transformed into nonlinear ordinary differential equations. The highly nonlinear problem is then solved by homotopy analysis method. Effects of the various parameters are examined. The following conclusions can be drawn as a result of the analytical solution:

1. The velocity profile decreases with increase in *Re* in case of Renolds model.
2. In case of Renolds model the velocity profile decreases with increase in *A*.
3. In Vogel's model the temperature profile decreases with increase in *Re*.
4. Reynolds number *Re* and *A* lead to decrease the velocity profile in Vogel's model.
5. The velocity profile in Vogel's model increases with increase in *S*.
6. In case of Vogel's model the velocity profile increases with increase in *q*.
7. *L* leads to increase the velocity profile in Vogel's model.

References

[1] M. Massoudi, I. Christie, Effect of variable viscosity and viscous dissipation on the flow of a third grade fluid in a pipe, Int. J. Non-Lin. Mech. 30 (1995) 687–699.

[2] T. Hayat, R. Ellahi, S. Asghar, The influence of variable viscosity and viscous dissipation on the non-Newtonian flow: an analytic solution, Commun. Nonlin. Sci. Numer. Simulat. 12 (2007) 300–313.

[3] M. Yurusoy, M. Pakdermirli, Approximate analytical solutions for flow of a third grade fluid in a pipe, Int. J. Non-Lin. Mech. 37 (2002) 187–195.

[4] M. Pakdermirli, B.S. Yilbas, Entropy generation for pipe flow of a third grade fluid with Vogel model of viscosity, Int. J. Non-Lin. Mech. 41 (2006) 432–437.

[5] S. Nadeem, M. Ali, Analytical solutions for pipe flow of a fourth grade fluid with Reynold and Vogl's models of viscosities, Commun. Nonlin. Sci. Numer. Simulat. 14 (2009) 2070–2090.

[6] S. Nadeem, T. Hayat, S. Abbasbandy, M. Ali, Effects of partial slip on a fourth grade fluid with variable viscosity: an analytical solution, Nonlin. Anal.: Real World Appl. 11 (2010) 856–868.

[7] S. Nadeem, N.S. Akbar, Effects of temperature dependent viscosity on peristaltic flow of a Jeffrey-six constant fluid in a non-uniform vertical tube, Commun. Nonlin. Sci. Numer. Simulat. 15 (2010) 3950.

[8] L.J. Crane, Flow past a stretching plate, Z. Angew. Math. Phys. 21 (1970) 645–647.

[9] F.K. Tsou, E.M. Sparrow, R.J. Goldstein, Flow and heat transfer in the boundary layer on a continuous moving surface, Int. J. Heat Mass Transf. 10 (1967) 219–235.

[10] L.E. Erickson, L.T. Fan, V.G. Fox, Heat and mass transfer on a moving continuous flat plate with suction or injection, Ind. Eng. Chem. Fund. 5 (1966) 19–25.

[11] A. Mucoglu, T.S. Chen, Mixed convection on inclined surfaces, ASME J. Heat Transf. 101 (1979) 422–426.

[12] L.G. Grubka, K.M. Bobba, Heat transfer characteristics of a continuous stretching surface with variable temperature, ASME J. Heat Transf. 107 (1985) 248–250.

[13] M.V. Karwe, Y. Jaluria, Fluid flow and mixed convection transport from a moving plate in rolling and extrusion processes, ASME J. Heat Transf. 110 (1988) 655–661.

[14] C.H. Chen, Laminar mixed convection adjacent to vertical, continuously stretching sheets, Heat Mass Transf. 33 (1988) 471–476.

[15] E.M. Abo-Eldahab, M. Abd El-Aziz, Blowing/suction effect on hydromagnetic heat transfer by mixed convection from an inclined continuously stretching surface with internal heat generation/absorption, Int. J. Therm. Sci. 43 (2004) 709–719.

[16] A.M. Salem, M. Abd El-Aziz, Effect of Hall currents and chemical reaction on hydromagnetic flow of a stretching vertical surface with internal heat generation/absorption, Appl. Math. Model. 32 (7) (2008) 1236–1254.

[17] M. Abd El-Aziz, Thermal-diffusion and diffusion-thermo effects on combined heat and mass transfer by hydromagnetic three-dimensional free convection over a permeable stretching surface with radiation, Phys. Lett. A 372 (3) (2007) 263–272.

[18] C.Y. Wang, Fluid flow due to a stretching cylinder, Phys. Fluids 31 (1988) 466–468.

[19] R. Ellahi, S. Afzal, Effects of variable viscosity in a third grade fluid with porous medium; an analytic solution, Commun. Nonlin. Sci. Numer. Simulat. 14 (2009) 2056–2072.

[20] M.Y. Malik, A. Hussain, S. Nadeem, T. Hayat, Flow of a third grade fluid between coaxial cylinders with variable viscosity, Z. Naturforsch. 64a (2009) 588–596.

[21] S.J. Liao, An analytic solution of unsteady boundary layer flows caused by an impulsively stretching plate, Commun. Nonlin. Sci. Numer. Simulat. 11 (2006) 326–339.

[22] S. Abbasbandy, The application of homotopy analysis method to nonlinear equations arising in heat transfer, Phys. Lett. A 360 (2006) 109–113 (S. Nadeem).

[23] N.S. Akbar, Effects of temperature dependent viscosity on peristaltic flow of a Jeffrey-six constant fluid in a non-uniform vertical tube, Commun. Nonlin. Sci. Numer. Simulat. 15 (2010) 3950.

[24] S. Nadeem, N.S. Akbar, Influence of heat and mass transfer on a peristaltic motion of a Jeffrey-six constant fluid in an annulus, Heat Mass Transf. 46 (2010) 485.

[25] S.A. Shehzad, Z. Abdullah, A. Alsaedi, F.M. Abbasi, T. Hayat, Thermally radiative three-dimensional flow of Jeffrey nanofluid with internal heat generation and magnetic field, J. Magn. Magn. Mater. 397 (2016) 108–114.

[26] S.A. Shehzad, F.E. Alsaadi, S.J. Monaquel, T. Hayat, Soret and Dufour effects on the stagnation point flow of Jeffery fluid with convective boundary condition, Eur. Phys. J. Plus 128 (2013) 1–15.